

Effects of the Stochasticity on Transport Properties in High- β LHD

Yasuhiro SUZUKI, Kiyomasa WATANABE, Hisamichi FUNABA,
Satrou SAKAKIBARA, Noriyoshi NAKAJIMA,
Nobuyoyshi OHYABU and LHD experiment group

National Institute for Fusion Science, Toki 509-5292, Japan

(Received 22 December 2008 / Accepted 27 May 2009)

Effects of the stochasticity of magnetic field lines on transport properties are investigated. In a high- β LHD plasma, the structure of field lines in the peripheral region becomes stochastic by finite- β effects but the finite pressure gradient exists in that region. The radial diffusion coefficient and the Kolmogorov length of stochastic field lines are estimated. In the stochastic region, the radial diffusion of stochastic field lines becomes large and the Kolmogorov length becomes short due to increasing β . In that region, the radial heat transport becomes large due to the stochasticity of field lines.

© 2009 The Japan Society of Plasma Science and Nuclear Fusion Research

Keywords: LHD, high- β , HINT2, stochasticity, radial heat diffusivity

DOI: 10.1585/pfr.4.036

1. Introduction

Generating and keeping clear flux surfaces are aims of magnetic confinement researches, because the stochasticity of magnetic field lines leads the degradation of the confinement connecting between core and edge regions. There are some analytical works investigating the impact of the stochasticity of magnetic field lines on the radial transport property [1–4]. In those works, Rechester and Rosenbluth pointed out the radial heat transport due to stochastic field lines relates to both the stochastic diffusion parallel and perpendicular to the magnetic field [1]. On the other hand, the stochasticity of field lines due to finite- β effects is an intrinsic property in stellarator/heliotron. Since the pressure-induced perturbed field breaks the symmetry of the field, the structure of magnetic field lines becomes stochastic, especially in the peripheral region. In order to aim stellarator/heliotron reactors, studies of the transport due to stochastic field lines are critical and urgent issues.

The LHD is an $L = 2/M = 10$ heliotron device. Up to now, three-dimensional (3D) magnetohydrodynamic (MHD) equilibria were studied using a 3D MHD calculation code, HINT/HINT2 [5, 6], which is an initial value solver based on the relaxation method without the assumption of nested flux surfaces. In Refs. [5, 6], it was predicted the field structure becomes stochastic due to increasing β . In addition, simulating HINT2, the finite pressure gradient ∇p can exist in the stochastic region [6]. If the plasma is collisional, where the electron temperature in the peripheral region is several tens of electron volts, the connection length is still long compared to the electron mean free path in the region [7]. That is, there is a possibility to keep the finite pressure on stochastic field lines. On the other hand, LHD experiments suggest the plasma pressure

spread over the region expected stochastically [8]. This suggests two possibilities. One is clear flux surfaces are kept in the finite- β field. Thus, the temperature profile changes smoothly toward peripheral region. Another is flux surfaces become stochastic but the stochastization affects the ‘transport’ in the peripheral region.

In this study, properties of 3D MHD equilibrium and the radial heat transport due to stochastic field lines in high- β LHD equilibria are ‘practically’ investigated in high- β LHD plasmas. In next section, using the HINT2 code [6], the degradation of flux surface quality due to finite- β effects is studied in a LHD configuration. Then, the diffusive property of stochastic field lines is practically studied using the analytical theory [1]. Lastly, results are briefly summarized and shown future subjects.

2. Degradation of Flux Surface due to Increasing β

Figure 1 shows Poincaré plot of field lines for the vacuum field ($Z > 0$: red) and a finite- β equilibrium ($Z < 0$: blue) and profiles of the connection length L_C along R on $Z = 0$ *const.* plane for an inward shifted configuration ($R_{ax} = 3.6$ m, $A_p = 5.8$, $\kappa \approx 1$), where A_p is the plasma aspect ratio and κ is an averaged elongation of the plasma cross section along the toroidal angle ϕ . The figure is plotted on horizontally elongated cross section. The volume averaged beta $\langle \beta \rangle_{dia}$ is about 3% and the initial pressure profile is set to $p = p_0(1 - s)(1 - s^4)$, where p_0 is the pressure on the magnetic axis and s is the normalized toroidal flux on the edge. This is a typical profile in high- β experiments. The total net toroidal current is assumed to zero as the net-current free equilibrium. In LHD experiments, achieved β depends on the preset axis position R_{ax} in the

author's e-mail: ysuzuki@LHD.nifs.ac.jp

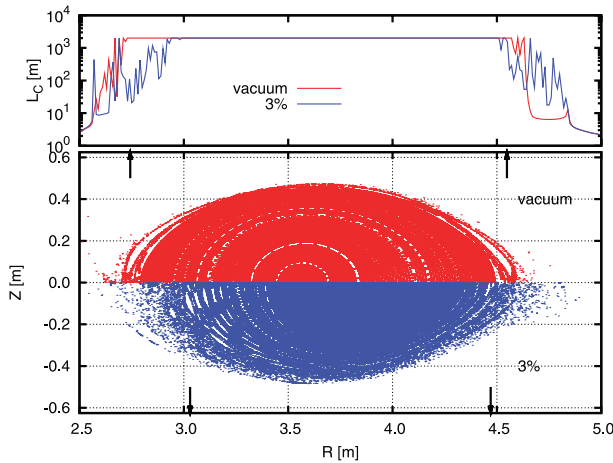


Fig. 1 Poincaré plots of vacuum field ($Z > 0$: red) and a finite- β equilibrium ($Z < 0$: blue) are shown in an inward shifted configuration ($R_{ax} = 3.6$ m, $A_p = 5.8$, $\kappa \approx 1$). Arrows indicate positions of well-defined LCFS on $Z = 0$ const. plane, respectively. Upper figure shows profiles of the connection length L_C along R on $Z = 0$ const. plane.

vacuum and 3.6 m is the standard in high- β operation. For the vacuum, clear flux surfaces are kept in the peripheral region. However, for finite- β , the last closed flux surface (LCFS) shrinks than the vacuum one and the field lines become stochastic in the peripheral region. In addition, small island chains on rational surfaces evolve. Arrows in Fig. 1 indicate positions of the LCFS on $Z = 0$ const. plane. The plasma volume with clear flux surfaces decreases about 25% due to the stochasticity of field lines. According to increasing the stochasticity of field lines, the profile of the connection length L_C changes and L_C becomes short in the stochastic region. However, in spite of increasing the stochasticity, L_C is still the order of 10^2 .

In Fig. 2, Poincaré plot of field lines ($Z > 0$: red), contour lines of the plasma pressure ($Z < 0$: blue) are plotted. As the reference, profiles of the electron temperature T_e in a typical shot (#46465, $t = 1.625$), the electron mean free path (emfp) λ_e estimated on the same shot and the connection length of field lines L_C are also shown along R on $Z = 0$ const. plane. Two arrows in the profile of T_e indicate positions of well-defined LCFS for the vacuum on $Z = 0$ const. plane. In figs, the plasma pressure exists in the peripheral region expected stochastically and contour lines keep closed surfaces in the stochastic region. The experiment suggests existence of T_e in the stochastic region. The physics of the existence of T_e in the stochastic region is proposed as following. Usually, in high- β experiment of LHD, since the plasma is the collisional plasma with low magnetic field and low temperature, the λ_e is shorter than L_C in the peripheral region. From the viewpoint of the transport, this means the stochastic field line can keep the finite pressure gradient ∇T_e in the peripheral region.

The equilibrium calculation suggests the stochastic-

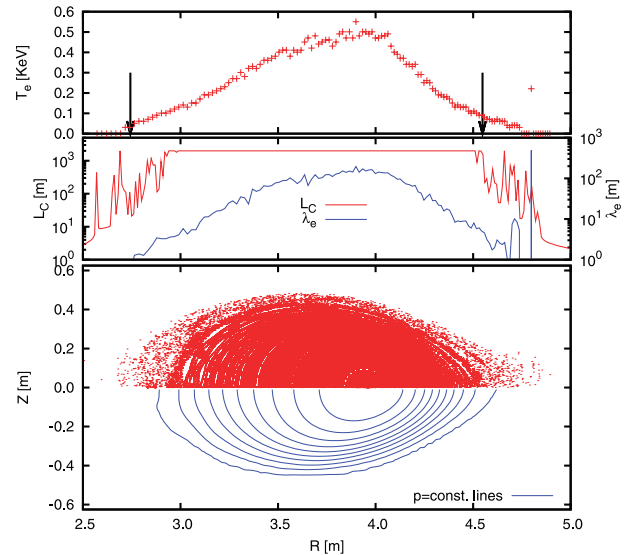


Fig. 2 Poincaré plot of magnetic field lines ($Z > 0$: red) and contour lines of the plasma pressure ($Z < 0$: blue), profiles of the electron temperature T_e (#46465, $t = 1.625$), the electron mean free path λ_e estimated on the same shot and the connection length of field lines L_C are also shown along R on $Z = 0$ const. plane. Two arrows in top figure indicate positions of well-defined LCFS for the vacuum on $Z = 0$ const. plane.

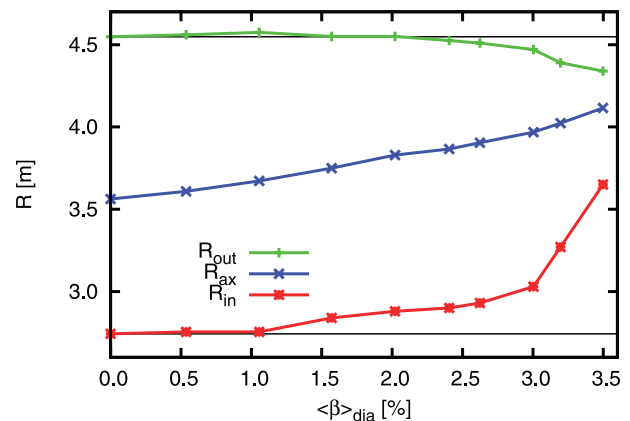


Fig. 3 The change of positions of inward (red) and outward (green) LCFS on horizontally elongated cross section is plotted as a function of $\langle \beta \rangle_{dia}$. The shift of the axis is also plotted for the reference (blue). All are plotted on $Z = 0$ const. plane

ity of magnetic field lines and existing ∇T_e in the stochastic region for the net-current free equilibrium. However, if the stochastic region increases widely, it is unclear either the stochastic region can keep ∇T_e or not. In order to study the degradation of flux surfaces due to increasing β , the change of the LCFS and magnetic axis is shown in Fig. 3 as the function of $\langle \beta \rangle_{dia}$. Three positions are plotted on $Z = const.$ plane corresponding to Fig. 2. At first, the change of the outward torus is considered. For low- β equilibria ($< 1\%$), the LCFS is almost fixed to the vac-

uum position. Then, increasing β ($> 1\%$), the LCFS still sustains near the vacuum LCFS. For high- β ($> 2\%$), the LCFS shrinks due to increasing β . On the other hand, the inward region, the LCFS degrades monotonically due to increasing β . As a result, we guess the degradation of the transport is significantly important at high- β ($> 2\%$). The magnetic axis also monotonically changes due to increasing β . At a high- β ($\langle\beta\rangle_{\text{dia}} \sim 3\%$), the Shafranov shift Δ/a achieves about 0.5. However, the MHD equilibrium does not collapse and it is sustained.

3. Radial Heat Diffusivity due to Stochastic Field Lines

The radial heat transport increases as it gains the stochasticity. In the collisionless plasma, where the electron mean free path λ_e is very long, the radial heat conductivity χ_r due to ‘only’ the stochasticity of magnetic field lines is given by

$$\chi_r = D_{\text{FL}} v_{\text{th}}, \quad (1)$$

where v_{th} is the electron thermal velocity and D_{FL} is the diffusion coefficient of magnetic field lines and defined by

$$D_{\text{FL}} = \frac{\langle\Delta r^2\rangle}{L_{\text{col}}}, \quad (2)$$

where L_{col} is the correlation length to calculate the diffusion coefficient. Since χ_r is the contribution of only the stochasticity of magnetic field lines, the effective radial transport χ_{eff} is given by

$$\chi_{\text{eff}} = \chi_r + \chi_{\perp}. \quad (3)$$

On the other hand, in the collisional plasma, Krommes *et al.* identifies three different subregimes with decreasing collisionality [4], which are fluid regime ($\tau_{\perp} < \tau_{\parallel} < \tau_k$), Kadomtsev-Pogutse ($\tau_{\perp} < \tau_{\parallel} < \tau_k$) and Rechester-Rosenbluth ($\tau_{\perp} < \tau_{\parallel} < \tau_k$) regime, where $\tau_{\parallel} = L_0^2/\chi_{\parallel}$, $\tau_k = L_k^2/\chi_{\parallel}$ and $\tau_{\perp} = 1/(k_{\perp}^2 \chi_{\perp})$. In typical parameters of LHD experiments, the collisionality is expected the Rechester-Rosenbluth (RR) regime in the region expected stochastically because $\chi_{\parallel}/\chi_{\perp} \sim 10^6$ [9–11]. The radial heat conductivity due to the stochasticity of field lines is given by

$$\chi_r = D_{\text{FL}} \chi_{\parallel} / L_k \quad (4)$$

in the RR regime, where L_k is the Kolmogorov length. The Kolmogorov length L_k is a characteristic parameter to measure the stochasticity. Thus, Eq. 4 means the parallel contribution of the stochasticity is very important as well as the perpendicular contribution, because L_k plays the role of the correlation length along field lines.

As above mentioned, to estimate χ_r , D_{FL} and L_k are necessary. The question is how to calculate those values. In this study, we use following procedure to calculate D_{FL}

of field lines; (i) the distribution of the normalized toroidal flux $s = \Phi/\Phi_{\text{edge}}$ is given at first, where Φ is calculated by integrating inside contour lines at $p = \text{const.}$ (ii) then, the normalized minor radius ρ is calculated and field lines are traced from distributed points on $\rho = \text{const.}$ plane. (iii) in the last, the mean squared displacement of $\langle\Delta\rho^2\rangle$ is calculated with tracing field lines along L and the distribution coefficient is given by

$$D_{\text{FL}} = \frac{r_{\text{eff}}^2 \langle\Delta\rho^2\rangle}{L_{\text{col}}}, \quad (5)$$

where r_{eff} is the effective minor radius. To estimate the radial diffusion using the mean squared displacement, the definition of the radial coordinate is very important. In tokamak studies of the Dynamic Ergodic Divertor (DED) [12, 13], the radial coordinate is defined by 2D MHD equilibrium field because they use the vacuum approximation, which is 2D MHD equilibrium superposed the perturbed field for the vacuum. It is an easy way to calculate the radial displacement. However, that approximation does not include the plasma response on the perturbation field. In this study, since we have the 3D MHD equilibrium field obtained from the HINT2, we use the averaged plasma pressure to integrate the toroidal flux Φ . The averaged plasma pressure is calculated reproducing the experimental observation using HINT modeling (see Appendix). On the other hand, in tokamaks, the Kolmogorov length is given by the quasi-linear form [4], which is connected to the Chirikov parameter because the external perturbations are given. However, since the stochasticity in stellarator/heliotron plasmas is driven by the pressure-induced perturbation, the mode number and its amplitude of perturbations are unclear and the calculation of those values is very difficult. We have 3D MHD equilibrium field including all modes of pressure-induced perturbations but the Fourier decomposition of those perturbations on the stochastic field is difficult because of the radial coordinate. Thus, we estimate the Kolmogorov length using a following definition,

$$d = d_0 \exp\left(\frac{l}{L_k}\right), \quad (6)$$

where d is the circumference of small flux tube and l is the length of the flux tube. Using this definition, the impact finite- β effects on L_k is studied in vacuum configurations in LHD [8] and finite- β equilibria in Wendelstein 7-X [14].

In Fig. 4, profiles of D_{FL} and $1/L_k$ are plotted. The Kolmogorov length $1/L_k$ is plotted as the inverse to compare the change of D_{FL} . Detailed Poincaré plot of field lines and the profile of L_C are also plotted for the reference. Colors indicates starting points of field line tracing as following; red is $4.3 \text{ m} < R < 4.48 \text{ m}$ and for $R > 4.48 \text{ m}$ color changes at each 2 cm from green, blue, purple, light blue, yellow, black and orange. D_{FL} is very small in clear flux surfaces. However, in the stochastic region, the diffusion coefficient increases along R . In Poincaré plot, field

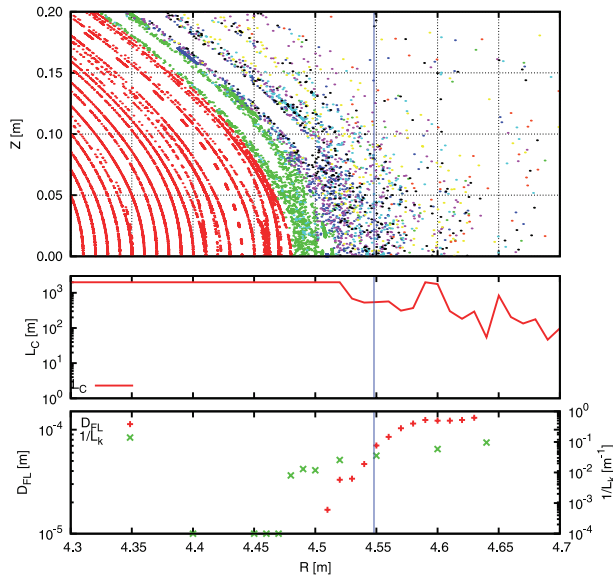


Fig. 4 Profiles of the connection length L_C , the diffusion coefficient of field lines D_{FL} and the inverse of Kolmogorov length $1/L_k$ are plotted along R ($4.3 < R < 4.7$). Poincaré plot of field lines is also plotted for the reference. Blue lines in figs indicate outermost position of LCFS for the vacuum.

lines with colored green becomes slightly stochastic and turn around with small width along the toroidal direction. At $R > 4.5$ m, field lines overlap between both side and become perfectly stochastic. However, in the stochastic region, D_{FL} is relatively small $\sim 10^{-4}$. On the other hand, the inverse of the Kolmogorov length rapidly becomes exponentially short along R and the jump appears near the LCFS. This suggests the parallel correlation length is more sensitive than the perpendicular direction. In the outermost position calculated ($R = 4.64$ m), L_k is about 11 m.

As discussed in previous section, the Shafranov shift Δ/a achieved to about 0.5 in the inward shifted configuration. In order to achieve higher β , the reduction of the shift is necessary. An aspect to reduce the shift is the control of the plasma aspect ratio A_p . In LHD experiments, the optimization of the plasma aspect ratio had done. For $A_p = 6.6$, the diamagnetic β achieved 4.8% in the quasi-steady state operation. In Fig. 5, Poincaré plots of field lines in an optimized configuration ($A_p = 6.6$) are plotted for the vacuum ($Z > 0$: red) and a finite- β equilibrium ($Z < 0$: blue). The volume averaged beta $\langle \beta \rangle_{dia}$ is 4.8% in the equilibrium. Though the achieved β is relative high, the shift of the axis is smaller than the inward shifted configuration. However, the magnetic field lines become stochastic and island chains evolve. In Fig. 6, profiles of D_{FL} and $1/L_k$ in the optimized configuration are plotted corresponding to Fig. 4. Comparing Fig. 4, the increase of D_{FL} is relatively large. However, $1/L_k$ is almost same. The jump of $1/L_k$ also appears but the jump is the inside on islands. Since D_{FL} is relatively large than the inward shifted configura-

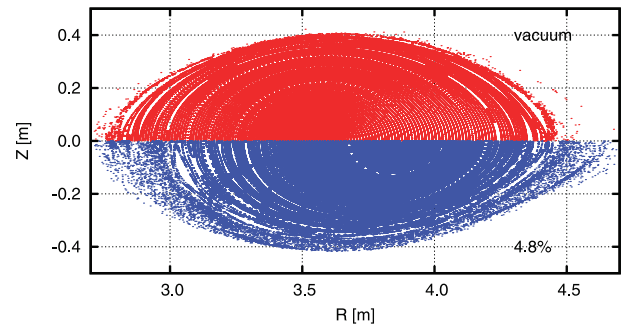


Fig. 5 Poincaré plots of magnetic field lines for the vacuum field ($Z > 0$: red) and a finite- β equilibrium ($Z < 0$: blue) are plotted in an optimized configuration ($R_{ax} = 3.6$ m, $A_p = 6.6$, $\kappa \approx 1$).

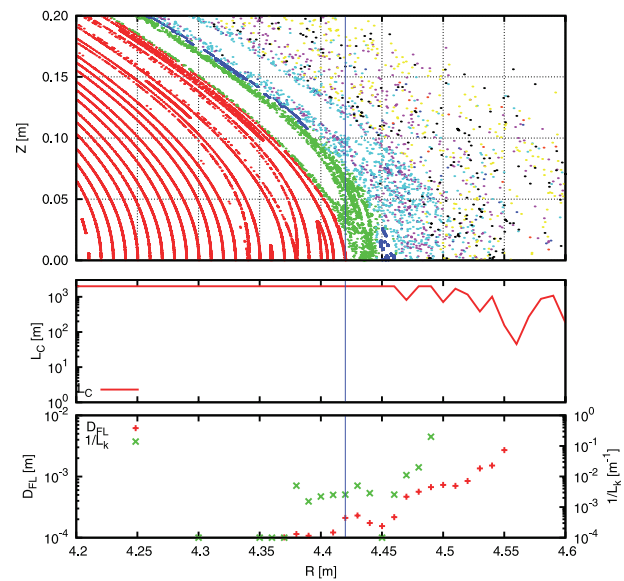


Fig. 6 Profiles of the connection length L_C , the diffusion coefficient of field lines D_{FL} and the inverse of Kolmogorov length $1/L_k$ are plotted for an optimized configuration as corresponding to Fig. 4. Poincaré plot of field lines is also plotted for the reference. Blue lines in figs indicate outermost position of LCFS for the vacuum.

tion, the degradation of the transport is expected.

Finally, we estimate the radial heat conductivity χ_r due to only the stochasticity of field lines from above consideration. In Fig. 7, radial profiles of the electron temperature T_e and density n_e in the typical shot (#61962) corresponding to Fig. 3 are shown at $4.3 \text{ m} < R < 4.7$ m. A dashed line indicates the outermost position of the LCFS on $Z = 0$ *const.* plane. The finite T_e and n_e exist over the vacuum LCFS although field lines become stochastic in that region. From T_e and n_e in the shot, the radial heat conductivity χ_r is estimated with D_{FL} and L_k in Fig. 4. Here, $\chi_{||}$ is defined by following equation [15],

$$\chi_{||} = 3.16 \frac{n_e T_e \tau_e}{m_e} \quad (7)$$

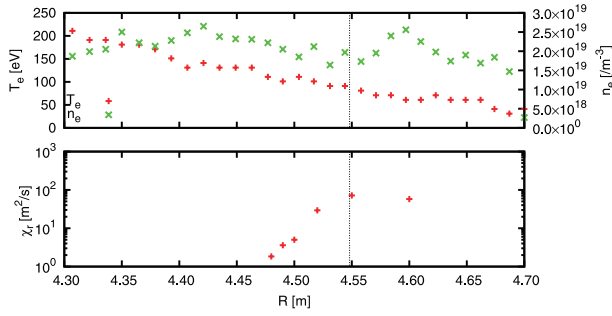


Fig. 7 Profiles of the electron temperature T_e and density n_e are plotted for the inward shifted configuration along $R(4.3 < R < 4.7)$ on $Z = 0$ const. plane. The profiles of the electron heat conductivity χ_r due to only the stochasticity of field lines is also plotted.

and

$$\tau_e = \frac{3\sqrt{m_e}T_e^{3/2}}{4\sqrt{2\pi}\lambda e^4 Z^2 n_e}. \quad (8)$$

Of course, χ_r is almost zero in the core with closed flux surfaces. However, in the stochastic region, χ_r increases with D_{FL} and $1/L_k$. At $R = 4.55$ m, χ_r becomes nearly 10^2 [m²/s]. In Ref. [16], the local transport χ_{eff} in the plasma core was discussed. In that study, χ_{eff} is about 1 [m²/s] at $R < 4.5$ m. There is still keeping clear flux surfaces. Thus, this result is not inconsistent to the experiment but insufficient to compare the experiment. In order to compare χ_r with the experimental data, it is necessary to analyze the local transport in the stochastic region ($R > 4.5$ m). The comparison of that and other estimation, which are obtained from the transport code for the edge plasma [9, 17], is a future subject. In tokamaks, it is pointed out that the RR formulation is larger than results of simulated studies [12, 13]. The confirmation of the RR formulation is another subject.

4. Summary

The stochasticity of magnetic field lines and effects on the transport properties due to finite- β effects are investigated in net-current free equilibria. Flux surfaces keep clear structure until the intermediate- β ($< 2\%$). However, for high- β , flux surfaces rapidly degrade due to the increased β . Characteristic properties, which are the diffusion coefficient of magnetic field lines and the Kolmogorov length, are estimated. In a high- β equilibrium, stochastic properties appear in the edge. Using Rechester-Rosenbluth formulation, the radial heat diffusivity due to only the stochasticity of magnetic field lines is estimated. The estimated diffusivity is very large. In this study, estimated L_k is shorter than L_C . This suggests a possibility that the theory to consider this plasma is not the Rechester-Rosenbluth [1] but the fluid model [4]. Anyways, since the Kolmogorov length is estimated from limited equilibria, it is necessary

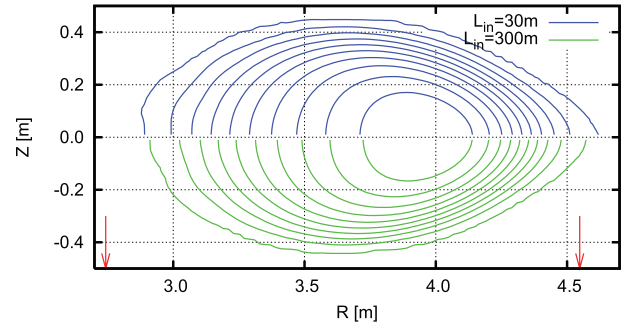


Fig. 8 Contour lines with different L_{in} ($Z > 0$ and $Z < 0$) are shown at the plane corresponding to Fig. 1. Blue lines indicate contour lines with $L_{in} = 30$ m and green lines indicate $L_{in} = 300$ m. Contour lines in the edge are different.

further studies.

In addition, we consider only the net-current free equilibrium. In recent LHD experiments, spontaneous evolution and suppression of the magnetic island were observed [18–20]. This suggests a possibility that stochastic field lines are recovered by the plasma itself, so-called ‘self-healing’ [21]. With considering only the Pfirsch-Schlüter (P-S) current, flux surfaces in the peripheral region become stochastic in this study. However, the self-healing by the noninductive current like the bootstrap current was proposed [22]. The study including that is another future subject.

A. HINT modeling

The HINT2 calculates converged pressure distribution in the finite- β field by

$$p^{i+1} = \bar{p} = \frac{\int_{-L_{in}}^{L_{in}} \mathcal{F} p^i \frac{dl}{B}}{\int_{-L_{in}}^{L_{in}} \frac{dl}{B}}, \quad \mathcal{F} = \begin{cases} 1 & \text{for } L_C \geq L_{in} \\ 0 & \text{for } L_C < L_{in} \end{cases} \quad (9)$$

where, i means a step number of iterations, L_C is the connection length of a magnetic field line starting each grid point (L_C is finite for open magnetic field lines), and L_{in} is prescribed as an input parameter to control the calculation. Equation 9 calculates the ‘averaged’ plasma pressure on the flux tube. This corresponds to simulate the radial diffusion of field lines. In order to consider this effects, profiles of plasma pressure with different L_{in} ($=30$ m and 300 m) are shown in Fig. 8. For $L_{in} = 300$ m, contour lines are different, especially in the stochastic region. If the distance along B is shorter than L_{in} , the averaged pressure \bar{p} is set to zero. In Fig. 2, since L_C is $10^1 \sim 10^2$ m, the distribution of \bar{p} is sensitive to L_{in} . This study has an assumption that the electron temperature is low because of the consideration of high- β experiments (see Fig. 2). Thus, we adopt L_{in} is 30 m.

Acknowledgment

The authors would like to thank Drs. M. Kobayashi, R. Kanno, S. Satake, A.H. Reiman, M.C. Zarnstorff, A. Weller, J. Geiger for fruitful discussion. This work is performed with the support and under the auspices of the NIFS Collaborative Research Program (NIFS06KTAT023, NIFS06KLHH303). This work was supported by Grant-in-aid for Scientific Research for Young Scientists (B) 20760585 from the Ministry of Education, Culture, Sports, Science and Technology.

- [1] A.B. Rechester and M.N. Rosenbluth, *Phys. Rev. Lett.* **40**, 38 (1978).
- [2] T.H. Stix, *Nucl. Fusion* **18**, 353 (1978).
- [3] B.B. Kadomtsev and O.P. Pogutse, in *Proc. 7th Int. Conf. Fusion energy*, Innsbruck 1978 (International Atomic Energy Agency, Vienna, 1979), Vol. 1, p.649.
- [4] J.A. Krommes *et al.*, *J. Plasma Phys.* **30**, 11 (1983).
- [5] T. Hayashi *et al.*, *Phys. Fluids B* **2**, 329 (1990).
- [6] Y. Suzuki *et al.*, *Nucl. Fusion* **46**, L19 (2006).
- [7] K.Y. Watanabe *et al.*, *Plasma Phys. Control. Fusion* **49**, 605 (2007).
- [8] T. Morisaki *et al.*, *J. Nucl. Matter.* **313-316**, 548 (2003).
- [9] Y. Feng *et al.*, *Nucl. Fusion* **48**, 024012 (2008).
- [10] Q. Yu, *Phys. Plasmas* **13**, 062310 (2006).
- [11] M. Hölzl *et al.*, *Phys. Plasmas* **14**, 052501 (2007).
- [12] M. Kobayashi *et al.*, *Nucl. Fusion* **44**, S64 (2004).
- [13] Ph. Ghendrih *et al.*, *Nucl. Fusion* **42**, 1221 (2002).
- [14] E. Strumberger, *Contrib. Plasma Phys.* **38**, 106 (1998).
- [15] V.D. Shafranov *et al.*, *Sov. J. Plasma Phys.* **2**, 99 (1976).
- [16] H. Funaba *et al.*, *Plasma Fusion Res.* **3**, 022 (2008).
- [17] M. Kobayashi *et al.*, *Plasma Fusion Res.* **3**, S1005 (2008).
- [18] K. Narihara *et al.*, *Phys. Rev. Lett.* **87**, 135002 (2001).
- [19] N. Ohyaabu *et al.*, *Phys. Rev. Lett.* **88**, 055005 (2002).
- [20] Y. Narushima *et al.*, *Nucl. Fusion* **48**, 075010 (2008).
- [21] T. Hayashi *et al.*, *Phys. Plasmas* **1**, 3262 (1994).
- [22] C.C. Hegna and J.D. Callen, *Phys. Plasmas* **1**, 3135 (1994).